

# Observations on CFD Verification and Validation from the AIAA Drag Prediction Workshops

Joseph H. Morrison\* and Bil Kleb†

*NASA Langley Research Center, Hampton, VA, Zip 23681*

and

John C. Vassberg‡

*The Boeing Company, Huntington Beach, CA, 92647*

The authors provide observations from the AIAA Drag Prediction Workshops that have spanned over a decade and from a recent validation experiment at NASA Langley. These workshops provide an assessment of the predictive capability of forces and moments, focused on drag, for transonic transports. It is very difficult to manage the consistency of results in a workshop setting to perform verification and validation at the scientific level, but it may be sufficient to assess it at the level of practice. Observations thus far: 1) due to simplifications in the workshop test cases, wind tunnel data are not necessarily the “correct” results that CFD should match, 2) an average of core CFD data are not necessarily a better estimate of the true solution as it is merely an average of other solutions and has many coupled sources of variation, 3) outlier solutions should be investigated and understood, and 4) the DPW series does not have the systematic build up and definition on both the computational and experimental side that is required for detailed verification and validation. Several observations regarding the importance of the grid, effects of physical modeling, benefits of open forums, and guidance for validation experiments are discussed. The increased variation in results when predicting regions of flow separation and increased variation due to interaction effects, e.g., fuselage and horizontal tail, point out the need for validation data sets for these important flow phenomena. Experiences with a recent validation experiment at NASA Langley are included to provide guidance on validation experiments.

## Nomenclature

$C_D, CD$	drag coefficient
$C_L, CL$	lift coefficient
$C_M, C_m, CM$	pitching moment coefficient
$C_v$	coefficient of variation, $\hat{\sigma}/\hat{\mu}$
$d$	diffuser throat diameter
$h$	one-dimensional estimate of grid spacing
$i_H$	horizontal tail incidence angle, degrees
$L$	length of recirculation region
$M$	Mach number
$N, NPTS$	number of solution points in a mesh
$p$	order of accuracy of numerical scheme
$Re$	Reynolds number based on reference chord
$x, y, z$	Cartesian coordinates

### *Symbols*

$\alpha$	angle of attack, degrees
$\hat{\mu}$	estimate of the population mean
$\hat{\sigma}$	estimate of the population standard deviation

---

\*Branch Head, Computational AeroSciences Branch, Mail Stop 128, AIAA Associate Fellow.

†Assistant Branch Head, Computational AeroSciences Branch, Mail Stop 128, AIAA Senior Member.

‡Boeing Technical Fellow, AIAA Fellow.

## I. Introduction

OVER a decade ago, Computational Fluid Dynamics (CFD) became an integral tool for analysis and design in the aircraft industry. Since then, CFD's role has expanded beyond the prediction of attached flow at the cruise design condition to more complex flow physics at off-design conditions. The AIAA CFD Drag Prediction Workshop (DPW) began the current series of workshops to evaluate the state of the art in CFD. DPW has evolved with the application of CFD to ever more complex flows of industrial interest.

The DPW Series was initiated by a working group of members from the AIAA Applied Aerodynamics Technical Committee. For five workshops to date, the DPW Organizing Committee has adhered to a set of primary objectives:

- Assess state-of-the-art CFD methods as practical aerodynamic tools for the prediction of forces and moments on industry-relevant geometries, with a focus on absolute drag.
- Provide an impartial international forum for evaluating the effectiveness of CFD Navier-Stokes solvers.
- Promote balanced participation across academia, government labs, and industry.
- Use common public-domain subject geometries, simple enough to permit high-fidelity computations.
- Provide baseline grids to encourage participation and help reduce variability of results.
- Openly discuss and identify areas needing additional research and development.
- Conduct rigorous statistical analyses of CFD results to establish confidence levels in predictions.
- Schedule open-forum sessions to further engage interaction among all interested parties.
- Maintain a public-domain accessible database of geometries, grids, and results.
- Document workshop findings; disseminate this information through publications and presentations.

DPW was envisioned to assess state-of-the-art CFD methods for prediction of aerodynamic flows of industrial interest. DPW was not planned as a verification and validation study. The primary tool of DPW is code-to-code comparison on a transonic transport aircraft problem of interest. Code-to-code comparison is used to evaluate how results differ, not as a verification study (see Oberkampf and Roy<sup>1</sup> for restrictions on using code-to-code comparison for code verification). DPW was intended as a measure of the state-of-the-art and was expected to identify some CFD topics that would require further investigation to improve the state-of-the-art. However, the code-to-code variation between the participants in the first DPW was substantially larger than expected.<sup>2,3</sup> The following four workshops were largely devoted to identifying and understanding the sources of variation with an expectation to reduce the variation between submitted results. To reduce the variation, the organizing committee added various elements of verification to the workshops. For example, the fifth and most recent workshop added solution verification of turbulence models on simple 2D configurations.

The DPW series has consistently made approximations to modeling of the wind tunnel test that prevent the CFD predictions from being validated with the wind tunnel data. These approximations were made to increase participation and simplify the code-to-code comparisons. Wind tunnel data has been used as a guide to understand differences in CFD predictions. Several differences in CFD predictions were identified in the DPW Series that will require additional validation data to discriminate between results.

This paper presents some observations from the series of five Drag Prediction Workshops that represent a tremendous amount of work from an international cast of collaborators. Each workshop has generated open discussions and a series of side studies to investigate various issues identified in the workshop. There is no attempt here to provide a thorough review of all of the DPW results and follow-on studies. However, many of the results and observations below are pulled from this rich set of studies. The DPW series has also helped to identify the need for validation data for flow separation. Additional observations from a recent validation experiment conducted at NASA Langley are provided to guide possible validation experiments.

## II. DPW Background

DPW-I, held in June 2001<sup>2,3</sup> solicited CFD predictions of the lift, drag, and pitching moment for the DLR-F4 subsonic transport wing-body configuration. The DLR-F4 wing-body configuration<sup>4-6</sup> was chosen due to public availability of the geometry and experimental data from three wind tunnels. Test cases consisted of a single point solution at

a fixed value of  $C_L$ , calculation of a drag polar, and an optional calculation of drag rise at constant values of  $C_L$ . Grids were made available for participants, but DPW-I did not require a grid convergence study. A total of 38 solutions were submitted for the workshop from 18 participants using 13 different CFD codes. A summary of the results of DPW-I is given in Ref. 2, and a statistical analysis of the results is given in Ref. 3. The results of the code-to-code statistical analysis showed a disappointing 270 drag count spread in the fixed  $C_L$  data with a 100:1 confidence interval of more than  $\pm 50$  drag counts. (Industry's goal is  $\pm 1$  drag count.)

DPW-II, held in June 2003<sup>7,8</sup> focused on a grid refinement study and the prediction of installed pylon-nacelle drag increments. The DLR-F6<sup>9</sup> wing-body and wing-body-nacelle-pylon configurations were chosen for DPW-II since DLR and ONERA made data publicly available for this configuration. Test cases consisted of a single point solution at a fixed value of  $C_L$  and a drag polar for both the DLR-F6 wing-body and wing-body-pylon-nacelle configurations on coarse, medium, and fine grids. Optional test cases included a comparison of tripped and fully turbulent solutions and calculation of drag rise at fixed values of  $C_L$ . A total of 21 solutions were submitted for the workshop from 20 participants using 18 different CFD codes. There were 16 solutions that calculated all three grid levels for both the DLR-F6 wing-body and wing-body-pylon-nacelle from 15 participants using 15 different CFD codes. A summary of the results is given in Ref. 7, and a statistical analysis of the results is given in Ref. 8. The DLR-F6 configuration had substantial areas of separation at the wing-body juncture and at the wing-pylon juncture. Additionally, there was a region of separation at the trailing edge of the wing. The code-to-code scatter for the wing-body configuration on the medium grid was significantly reduced compared to DPW-I, however, there was no significant change in code-to-code scatter with increasing grid density.<sup>8,10</sup>

The panel session discussion at the conclusion of DPW-II identified three suggestions for a third workshop: (1) the large regions of separation were a likely culprit for the lack of grid convergence; therefore cases should be chosen with minimal separation, (2) simpler cases were required to allow for better grid convergence studies and wider participation, and (3) blind studies were preferable where experimental data were not available a priori. Vassberg et al.<sup>11</sup> designed a side-of-body fairing for DLR-F6 to produce attached flow in the wing-body juncture. The fairing was designated the FX2B, and the configuration was referred to as the DLR-F6-FX2B. Additionally, two isolated wings, designated DPW-W1 and DPW-W2, were designed<sup>12</sup> to be a simple geometry with DPW-W2 a single point optimization of DPW-W1.

DPW-III, held in June 2006<sup>10,12</sup> focused on grid convergence studies and predicted increments for the DLR-F6 wing-body with and without the FX2B side-of-body fairing. The Reynolds number was increased from 3 to 5 million to minimize the trailing edge separation. Participants submitted solutions for DPW-III before the data for the FX2B fairing were collected in an experimental program at DLR and NASA.<sup>13</sup> Additional test cases included a drag polar at fixed Mach number and an optional Reynolds number scaling study. An optional grid convergence study included four grid levels for the DPW-W1 and DPW-W2 isolated wing cases and a drag polar at a fixed Mach number where the angle-of-attack was specified rather than specifying a fixed  $C_L$ . A summary of the DPW-III results is given in Ref. 12, and a statistical analysis is given in Ref. 10. The code-to-code scatter for the DLR-F6 wing-body case was essentially the same for the separated (DLR-F6 no fairing) and attached (DLR-F6 with FX2B fairing) flow conditions.<sup>10</sup> The code-to-code scatter for the wing alone cases was noticeably lower than the wing-body cases, especially on coarse grids, when the variation due to lift was accounted for in the drag (through variation in lift-to-drag ratio and idealized profile drag coefficient).<sup>10</sup>

DPW-IV, held in June 2009<sup>14,15</sup> focused on prediction of both absolute and differential drag levels for wing-body and wing-body-horizontal tail configurations that are representative of transonic transport aircraft. Cases included a grid convergence study and a downwash study including prediction of trimmed drag on the NASA Common Research Model (CRM) wing-body-horizontal tail configuration. Optional cases included a Mach sweep study at fixed  $C_L$  and a Reynolds number study. The CRM was a new wing-body-horizontal tail configuration, with and without nacelle-pylons, developed by the NASA Subsonic Fixed Wing (SFV) Aerodynamics Technical Working Group (TWG) in collaboration with the DPW Organizing Committee.<sup>16</sup> The CRM is representative of a contemporary high-performance transonic commercial transport. DPW-IV was a blind test. The workshop was held in June 2009 and the experimental data were collected in the NASA Langley National Transonic Facility in January–February 2010 and in the NASA Ames 11-ft wind tunnel during March–April 2010.<sup>17,18</sup> A summary of the results from DPW-IV is provided in Ref. 14, and a statistical analysis of the results is given in Ref. 15.

The code-to-code scatter for the total drag, normalized by the total drag to account for different drag levels between cases, was virtually the same for DPW-II, DPW-III, and DPW-IV. The code-to-code variation of the forces and pitching moment, normalized by the appropriate force or pitching moment, was substantially larger on the horizontal tail component than on the wing or fuselage component. However, the scatter in the drag showed some reduction with increasing grid resolution.<sup>15</sup>

The panel discussion at the conclusion of DPW-IV recommended continuing the workshop series with continuing focus on the CRM and a grid convergence study using a common set of grids for all CFD codes. DPW-V, held in June 2012, focused on force and moment predictions for the CRM wing-body configuration, including a grid refinement study and an optional buffet study. The grid convergence study used a common grid sequence derived from a five block multiblock structured grid generated by Vassberg.<sup>19</sup> He generated six grid levels ranging from approximately 640 thousand grid points on the coarsest grid to over 138 million grid points on the finest mesh. This multi-block grid was converted to overset, unstructured hexahedral, unstructured prisms, and unstructured hybrid grids by using the exact same set of grid points. The grid convergence study required at least four of the six grid levels. Optionally, participants could include solutions on grids they developed. The results on this common grid sequence showed a clear reduction in variation of forces and moments<sup>20</sup> over previous workshops. The optional wing-body buffet study at fixed Mach used the medium grid from the common grid sequence at seven angles of attack. Some solutions exhibited a large side of body separation bubble not observed in the wind tunnel results at off-design or high angles of attack. An optional third case was a turbulence model verification case. This verification case identified some turbulence model implementation issues and a few outliers in the submissions. A summary of the results from DPW-V is given in Ref. 21, and a statistical analysis of the results is given in Ref. 20.

### III. Observations from DPW

The five Drag Prediction Workshops held to date provide a wealth of data on the state of CFD prediction of forces and moments for transonic transports. The workshops consist of participants presenting their results, summaries where all submitted results are plotted together, and extensive discussions. After the workshops, participants are provided an opportunity to submit additional results or to make corrections to results that were identified during the workshop. The process of a group of people from multiple institutions solving the same problem and plotting all of the results together is very powerful. The results at workshops were shared with the community at large through the DPW website<sup>22</sup> and special DPW-focused sessions organized at a conference typically six months or a year after the workshop. Additionally, many authors identified additional topics to study based on results of the workshop.

First, a little background on grid convergence and the asymptotic range is important. The test cases used in DPW-I through DPW-V are designed to compare results of different CFD predictions. To keep the workshops as general and open to as many participants both in terms of case complexity and computational cost, some simplifying assumptions are made. For example, cases are typically run fully turbulent rather than matching the experimentally specified transition location and calculations are specified as configurations in free air rather than modeling the wind tunnel and mounting system. The following section addresses these physical model approximations more fully. The result of these approximations is that the wind tunnel data is not necessarily the “correct” result that the prediction should match. Rather, the prediction should have an offset from the wind tunnel results that represents corrections for each of the effects that are not modeled. We therefore look at how the solutions from the CFD predictions compare to one another—an N-version test. Hensch<sup>3</sup> used a statistical approach that treated different computations as a collective and used N-version testing to investigate the submissions. No individual result is considered right or best. The statistical approach identified which solutions differed from the collective and was useful in identifying sources of variation.<sup>3,8,10,15,20</sup> Individual solutions could differ from the collective for multiple reasons. Different turbulence model, different numerical scheme, and errors are some of the sources of variation that were identified. Note, however, that understanding the reason for the variation is preferred over simply marking a solution as an outlier and ignoring it. Additionally, the mean of the solutions is occasionally used to investigate trends. However, it is not necessarily a better estimate of the “true” solution as it is merely an average of other solutions and has many coupled sources of variation. These studies provided a uniform method of evaluating trends in predictions over the course of the workshops.

Another tool that has been used since DPW-II is the grid convergence study. The variation between different CFD predictions has components due to the grid and numerical approximations (discretized equations, grid), physical modeling (e.g., turbulence model), and errors (i.e., approximations that affect the solution in unintended ways or that aren’t what the author intended). One of the goals of the workshop series is to identify these different sources of variation, understand their effect, and recommend sources that should be further studied to improve predictive capability. The grid convergence study provides a method to study the variation due to the grids and numerical approximations.

For a consistent numerical approximation of design order,  $p$ , the error will be reduced proportional to  $h^p$  as the grid is refined, where  $h$  is a measure of the grid size. Salas<sup>23,24</sup> has shown that the error is linear with  $h^p$  only if the grid is refined uniformly in all coordinate directions, e.g., if the grid spacing is halved in the  $x$  coordinate, it must also be halved in the  $y$  and  $z$  coordinates. Other factors such as low-order boundary conditions can also contribute to possible

non-linearity in the error. A grid convergence study reduces the numerical error thereby reducing variation between CFD predictions due to grids and numerical approximation to isolate physical modeling and error differences. If the discretization error is reduced by the aforementioned rate as the grid is uniformly refined in all coordinate directions, the grid is said to be in the asymptotic range for that set of discretized equations.

Baker<sup>25</sup> provides a physical interpretation of the asymptotic range as: all relevant flow features are captured to some degree on the target grid and further grid refinement only serves to sharpen their resolution. For Navier-Stokes computations this includes all shockwaves, expansions, vortex structures, boundary layers, wakes, and regions of flow separation. He further notes that the property of being in the asymptotic range is a function not only of the grid, but also of the set of discretized equations.

To compare the predictions of two different physical models, e.g., the Spalart-Allmaras and the Reynolds stress transport turbulence models, reducing the numerical error below the differences in the models becomes critical. Otherwise the differences are a non-linear interaction of the turbulence model and the numerical discretization errors and can be misleading when trying to draw conclusions about physical model performance.

An example of this can be seen in an axisymmetric example from Turgeon et al.<sup>26</sup> Figure 1 presents the length of the recirculation zone of the turbulent flow in a 30° axisymmetric diffuser obtained using an adaptive grid procedure with various numerical discretization schemes of the momentum and turbulence equations. All solutions are from

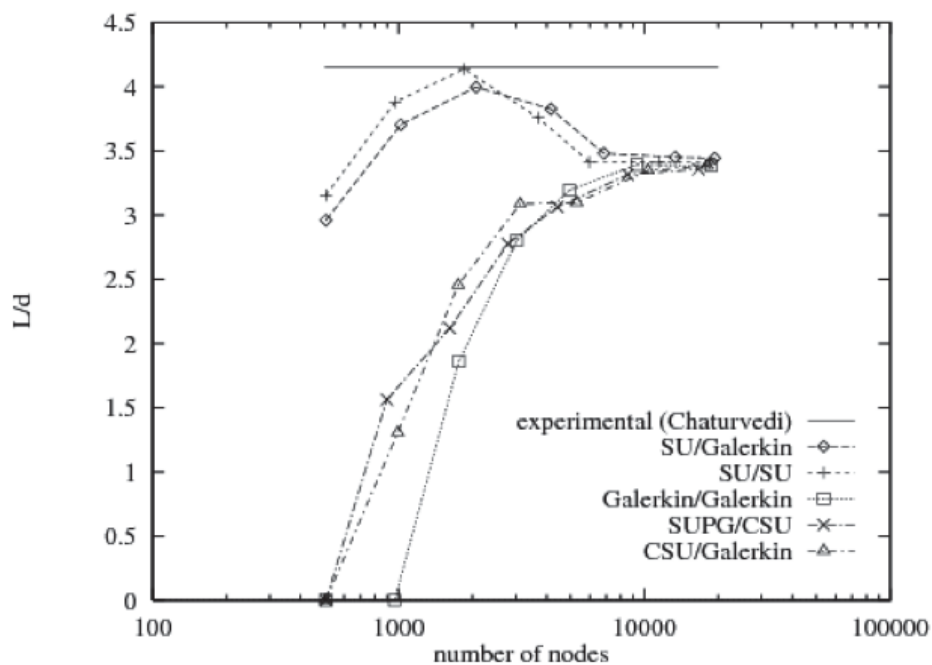


Figure 1: Recirculation length for 30° axisymmetric diffuser (from Turgeon et al.<sup>26</sup>).

the same CFD code with the same turbulence model. The variation between the solutions can be estimated using the range, which is clearly large on the coarse grids. As the grid is refined, the variation between the different numerical discretizations reduces until it eventually becomes zero on the finest grid where all of the discretizations give the same prediction of the recirculation length even though some of the discretizations completely miss the recirculation zone on the coarsest grids. The coarsest grid is not in the asymptotic range for the Galerkin/Galerkin, SUPG/CSU, and CSU/Galerkin discretizations since they predicted no recirculation. Since this is an adaptive grid sequence and not a uniform refinement, we don't expect to see the error necessarily decay as  $h^p$ . All discretizations converge to the same value of the recirculation length and the predictions are verified.<sup>27</sup> Only once the grid is converged can we accurately estimate the difference in the physical approximation.

The following sections summarize some of the key observations from the Drag Prediction Workshops. These are collected into three categories: grids and numerical approximations, physical modeling, and open forums.

## A. Grids and Numerical Approximations

After three workshops, the organizing committee recognized that a recurring theme of the workshop series was the importance of grid resolution and grid quality. Mavriplis et al.<sup>28</sup> provide an excellent review of grid issues in the

context of DPW-III results.

Two different studies of the DLR-F6 used in DPW-II demonstrate that the differences due to the grids is larger than differences due to physical modeling. Laflin et al.<sup>7</sup> noted that the series of coarse, medium, and fine grids used by the participants were of insufficient density to obtain asymptotic convergence of the solution. In addition to grid size, the four cases used in DPW-II also provided a means to evaluate the effect of boundary layer transition specification (fully turbulent versus fixed transition location), turbulence model, and grid type on the range of predicted drag data, but it was shown that, “[n]one of these appear to have as significant an effect as grid size.”<sup>7</sup>

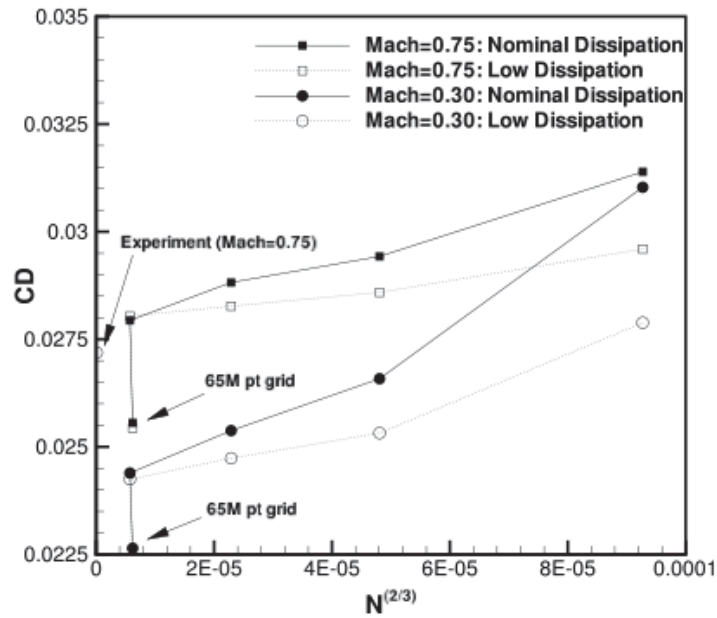
Mavriplis<sup>29</sup> performed a grid convergence and sensitivity study for the DLR-F6 wing-body used in DPW-II. Figure 2 shows the lift and drag coefficients calculated at a subcritical ( $M = 0.30$ ) and a transonic ( $M = 0.75$ ) condition at zero incidence. The calculations were performed using two different levels of numerical dissipation. A grid convergence study was performed on a self-similar grid sequence consisting 1 million, 3 million, 9 million, and 72 million grid points. The drag values appear to be converging asymptotically although the lift values still show a small oscillation in convergence on this grid sequence. However, when the same cases are computed on a 65 million grid point grid that was generated using a similar resolution but with a different topology, dramatically different results are obtained. The effect of the two different grid topologies is substantially stronger than the level of numerical dissipation and swamps the effects due to two other modeling considerations studied: the turbulence model distance function calculation and the thin-layer Navier-Stokes assumption.

Baker<sup>30</sup> applied the method developed in Baker<sup>25</sup> to evaluate whether results on the grid sequences used in DPW-II were in the asymptotic range. He identified nine of 23 submissions for the DLR-F6 wing-body that might be in the asymptotic range but only one of eight candidate submissions for the wing-body-nacelle-pylon. The remaining 21 of 31 submissions were clearly not in the asymptotic range. He identified grid deficiencies and insufficient iterative convergence, especially for the large regions of separation on the wing-body-nacelle-pylon, as potential reasons that submissions were not in the asymptotic range. None of the sequences that were candidates for being in the asymptotic range had a calculated order of accuracy that matched the design order of accuracy of the numerical approximation. The fact that the calculated order of accuracy did not match the design order is a potential indicator that the grids did not meet the uniform refinement criteria. In a workshop setting, ensuring that all solutions have been converged to an acceptable level to perform an “order-analysis” is difficult. Baker<sup>30</sup> also noted that the number of significant digits used in reporting measures of interest was insufficient for performing the order analysis. He recommended requiring additional significant digits in future workshops.

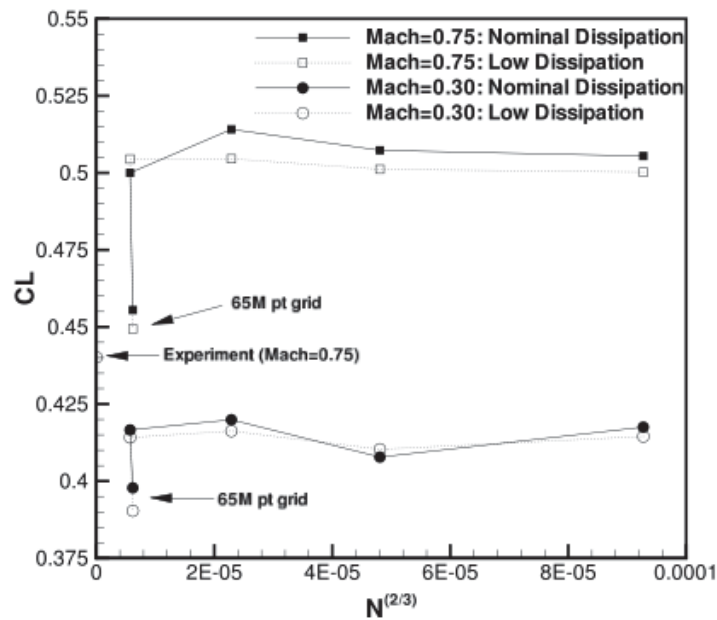
Eliasson et al.<sup>31</sup> examined the effect of grids on the side of body separation for the DPW-II DLR-F6 wing-body configuration. Calculations were made with the Edge solver with the same turbulence model ( $k-\omega$  EARSM) and the same numerical parameters; the only change was the grid families. Figure 3 shows a cut in the two grids at 15% wing span while Figure 4 shows the surface skin friction pattern at the wing-body junction for the two different unstructured grid families for three grid levels. A side of body separation bubble is visible for both the DLR grids and the ANSYS<sup>®</sup> grids. The separation on the ANSYS<sup>®</sup> grid is very small and weak. The separation on the DLR grid is a relatively extensive separation. The size of separation from the wind tunnel experiment appears to be between these two predictions. The separation region obtained with the DLR grids showed a better grid convergence in terms of its size and shape. The prediction of the separation region is clearly strongly influenced by the grid family; and so, from just these two solutions, determining which (if either) is the grid converged solution for the turbulence model is simply not possible.

Submissions for the DPW-III DLR-F6 wing-body configuration with and without FX2B fairing unanimously agreed that the flow was well attached for the FX2B configuration but had large variation in the predicted size of the separation bubble for the DLR-F6 without the fairing. Vassberg et al.<sup>12</sup> noted that the level to which the uniform refinement criterion of the grid families was achieved varied across the grids. An objective of DPW-III was to test a hypothesis that pockets of flow separation can be a root cause of poor grid-convergence characteristics. Although it appears that pockets of flow separation did adversely affect the grid-convergence trends of many of the CFD data blocks provided by participants, it did not seem to cause issues with others. The adverse grid convergence trends are possibly an indicator of poor resolution, poor grid quality of some flow regions, and/or non-uniformly refined grid families.

Sclafani et al.<sup>32</sup> demonstrated that the OVERFLOW code using structured overset grids achieved asymptotic convergence for the DPW-III DLR-F6 wing-body with FX2B fairing configuration and for the DPW-III DPW-W1/W2 wing-alone cases. Asymptotic grid convergence was demonstrated on the medium/fine/extra fine sequence of grids for both the FX2B and the wing-alone configurations but the coarse grid was not in the asymptotic range for either configuration. However, the DLR-F6 wing-body without the FX2B fairing had a large side of body separation region and did not exhibit asymptotic convergence—the side of body separation zone grew with increasing grid resolution.



(a) Computed lift.



(b) Computed drag.

Figure 2: Comparison of computed lift and drag coefficients for the DLR-F6 wing-body configuration versus number of grid points to the  $-2/3$  power for subsonic ( $M = 0.3$ ) and transonic ( $M = 0.75$ ) conditions at zero incidence on a sequence of uniformly refined grids and an alternate grid of 65 million points using the NSU3D solver (from Mavriplis<sup>29</sup>).

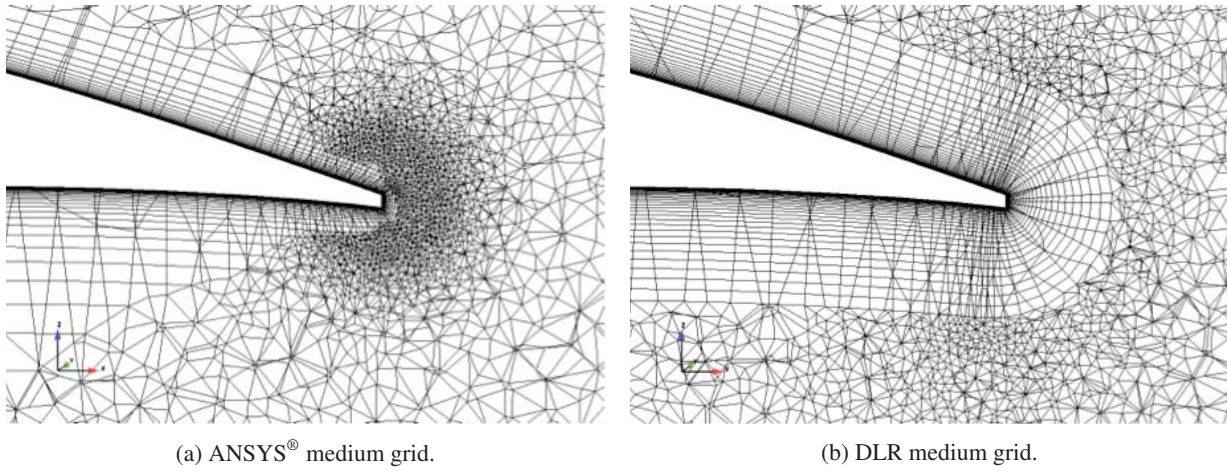


Figure 3: Grid cuts at 15% wing span for the DPW-II DLR-F6 wing-body configuration (from Eliasson et al.<sup>31</sup>).

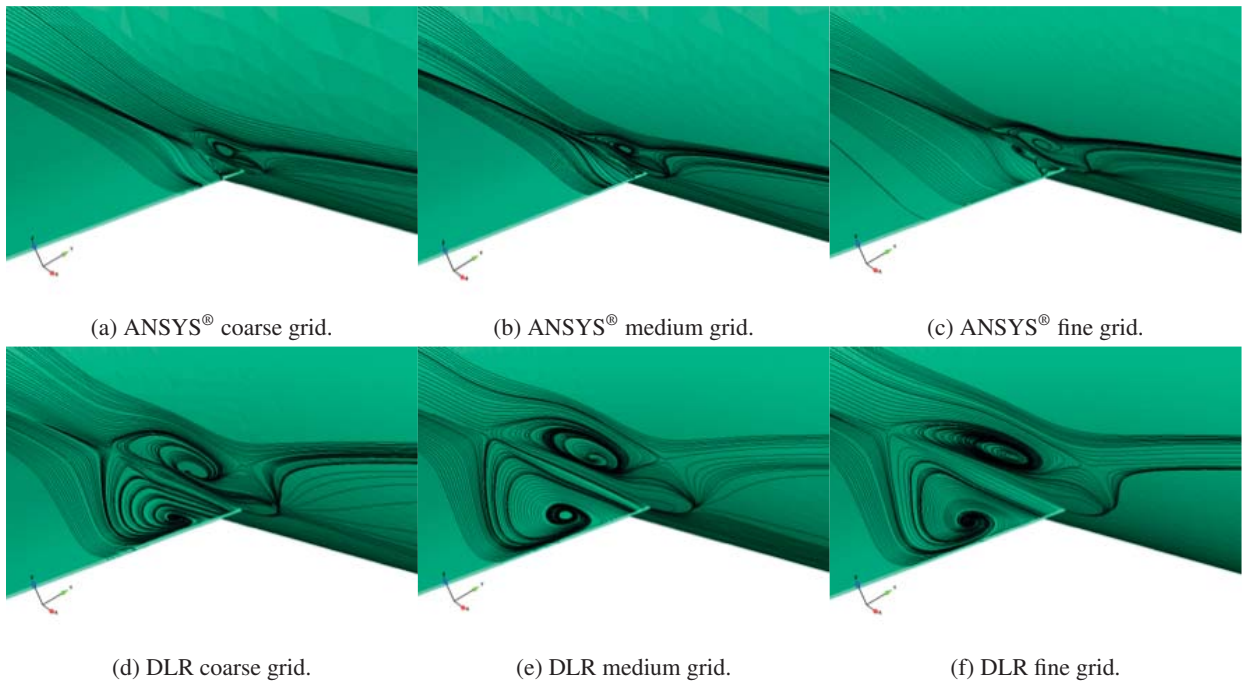


Figure 4: Surface friction pattern at wing-body junction from the ANSYS® and DLR grids at 1.23° angle of attack (from Eliasson et al.<sup>31</sup>).

Meanwhile, Tinoco et al.<sup>33</sup> and Murayama and Yamamoto<sup>34</sup> demonstrated relatively constant separation bubble size with increasing grid resolution on multiblock grids. Similarly, separation at the wing trailing edge varies from no separation predicted by Sclafani et al.<sup>32</sup> to an increase in trailing edge separation with increasing grid density by Mavriplis<sup>35</sup> on an unstructured mesh. See Mavriplis et al.<sup>28</sup> for further discussion of the variation in prediction of the flow separation regions. The DPW-III DLR-F6 results did not show a consistent trend: some work demonstrated no side of body separation, some work showed a constant separation bubble size with increasing grid resolution, and some work showed increasing separation bubble size with increasing grid resolution. Clearly the grid effects have not been completely resolved for this complex flow field and more work is required to resolve this issue.

The statistical summary for DPW-V<sup>20</sup> compared the grid convergence for DPW-II, DPW-III, DPW-IV, and DPW-V. The coefficient of variation of the total drag coefficient is plotted in Figure 5. The coefficient of variation,  $C_v$ , is used

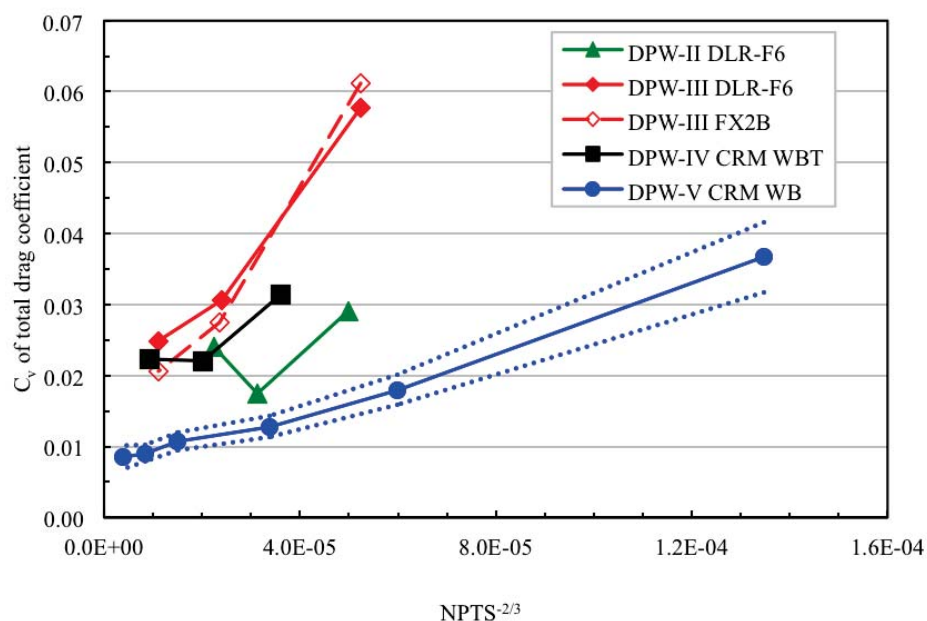


Figure 5: Coefficient of variation of total drag coefficient for DPW-II DLR-F6 wing-body, DPW-III DLR-F6 wing-body and DLR-F6 with FX2B fairing, DPW-IV CRM wing-body-horizontal tail, and DPW-V CRM wing-body (from Morrison<sup>20</sup>).

to compare variations from populations with different means. Figure 5 shows that the variation for DPW-II DLR-F6 wing-body, DPW-III DLR-F6 wing-body with and without FX2B fairing, and DPW-IV CRM wing-body-horizontal tail all have a similar level of variation. The variation for the DPW-III DLR-F6 wing-body solutions with and without the FX2B fairing are almost identical. The variation for the DPW-V CRM wing-body configuration has substantially lower variation than previous workshops. The dotted line plotted with the DPW-V CRM results is an estimate of the uncertainty in the variation due to the different number of results for each of the six grid levels. The reduced variation in DPW-V results is primarily due to the use of a common grid sequence.<sup>19</sup>

Through five workshops the grid has been a leading order effect on the solutions. Gridding guidelines were provided in an effort to use best practices and minimize variation due to grids. However, conformance to the gridding guidelines has been inconsistent and is very difficult to verify. For example, given a sequence of grids, how can we evaluate how uniform the refinement sequence is? Ollivier-Gooch<sup>36</sup> described an approach for analyzing whether two meshes are geometrically similar and therefore appropriate for a mesh refinement study. He calculated the size, anisotropy, and orientation of cells based on moments of the cells. He then projected these quantities from one mesh to another to enable comparison. The directions of the anisotropy were also compared. Ollivier-Gooch<sup>36</sup> examined a pair of meshes from DPW-III and showed that cells near the wing trailing edge and on the fuselage of the coarse mesh cells are somewhat smaller than a uniform refinement of those regions would produce. Overall there were more cells on the coarse mesh that were either slightly smaller or larger than would be expected from a uniform refinement. Tools such as this need further refinement and application to a wider range of grids to evaluate their effectiveness.

The workshops showed that the resolution and quality of grids affect the solution. Is there an a priori method

that can be used to estimate the quality of a solution on a given grid, which would enable improved grids before performing the CFD calculation? Dannenhoffer<sup>37</sup> investigated a priori grid metrics by using a 2D inviscid supersonic diamond airfoil. His systematic study computed the flow with more than 50 structured meshes and correlated a set of 30 grid quality metrics with seven measures of the solution error. A statistical analysis of the results showed that there was essentially no correlation of the a priori grid quality metrics with the measures of solution error. Dannenhoffer<sup>37</sup> concluded, “[t]his indicates that a priori ‘grid quality’ metrics can at most provide ‘loose guidance’ in the screening of computational grids.”

Cavallo and Feldman<sup>38</sup> extended the work of Ollivier-Gooch<sup>36</sup> to provide a more compact means of assessment and comparison of grid sequences and to allow solution pairs to be evaluated as a means of evaluating similarity and the asymptotic range. They evaluated the NASA Langley node-based tetrahedral mesh sequence from DPW-IV and observed that the mesh distributions were nearly identical between the coarse-medium pair and the medium-fine pair. This confirmed that this grid sequence forms a self-similar family of meshes.

Vos et al.<sup>39</sup> calculated the drag on the DPW-IV CRM by using both a near-field drag integration (integrating surface pressures and shear stresses) and a far-field drag integration procedure. They used the NSMB CFD solver with the same turbulence model and numerical parameters on six different multiblock grid sequences. They demonstrated approximately a 20 drag count variation between the multiblock grids with the near-field drag integration and about a 7 drag count variation between the solutions with the far-field drag integration. Using the far-field integration approach they were able to identify regions on several of the multiblock grids that accounted for an increase in error of the drag estimate: lack of grid clustering near the wing leading edge for the cfse-ra and Zeus grids; lack of grid clustering at the wing trailing edge for the cfse-ra, ANSYS<sup>®</sup>, and Zeus grids; and streamwise spacing that is too large on the wing for the ANSYS<sup>®</sup> grid.

Morrison<sup>20</sup> compared the forces and moments for each component (wing, fuselage, horizontal tail) of the DPW-IV DLR-F6 wing-body-horizontal tail and the DPW-V CRM wing-body configurations. Figure 6 shows that the total drag variation on the horizontal tail is approximately an order of magnitude larger than the variation on the fuselage. Also,

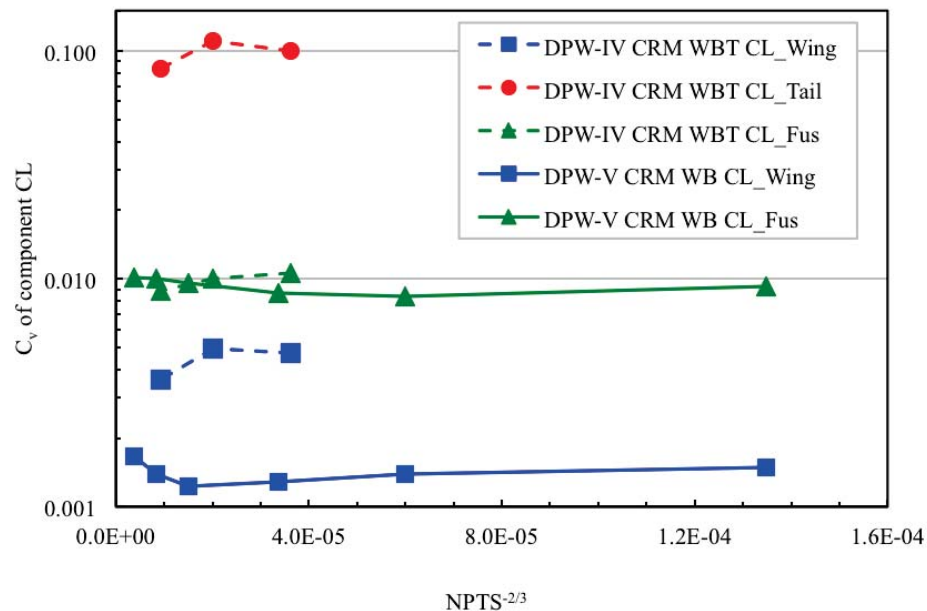


Figure 6: Coefficient of variation of lift coefficient for DPW-IV CRM wing, fuselage, and horizontal tail components and DPW-V CRM wing and fuselage components (from Morrison<sup>20</sup>).

the variation on the fuselage is approximately an order of magnitude larger than the variation on the wing. This tells us that differences between the total drag predictions is influenced more by the horizontal tail and the fuselage and infers that the grid resolution and grid quality is better on the wing and worse on the fuselage and tail. The lack of grid quality for the tail could be the grid over the horizontal tail and/or the wing wake grid which influences the inflow condition to the tail. This variation is possibly due to the state of the art in unstructured grid generation that tends to generate O-type grids around wing and tail surfaces, which leaves very coarse grids in the wakes. For such a grid topology, an

extreme amount of uniform refinement is required to reach the asymptotic range of the wake. Improvements to grids on the horizontal tail and fuselage components are also required to reduce the variation. Mavriplis et al.<sup>28</sup> also identified larger errors on the fuselage than the wing by examining the slope of the forces as a function of the average grid spacing. Lee-Rausch et al.<sup>40</sup> show similar trends for the DLR-F6 wing-body by using adjoint-based grid adaptation shown in Figure 7. In the figure, any non-blue color is a request for smaller grid spacing. Note the inset cut through the wing showing the request for more grid points in the wake.

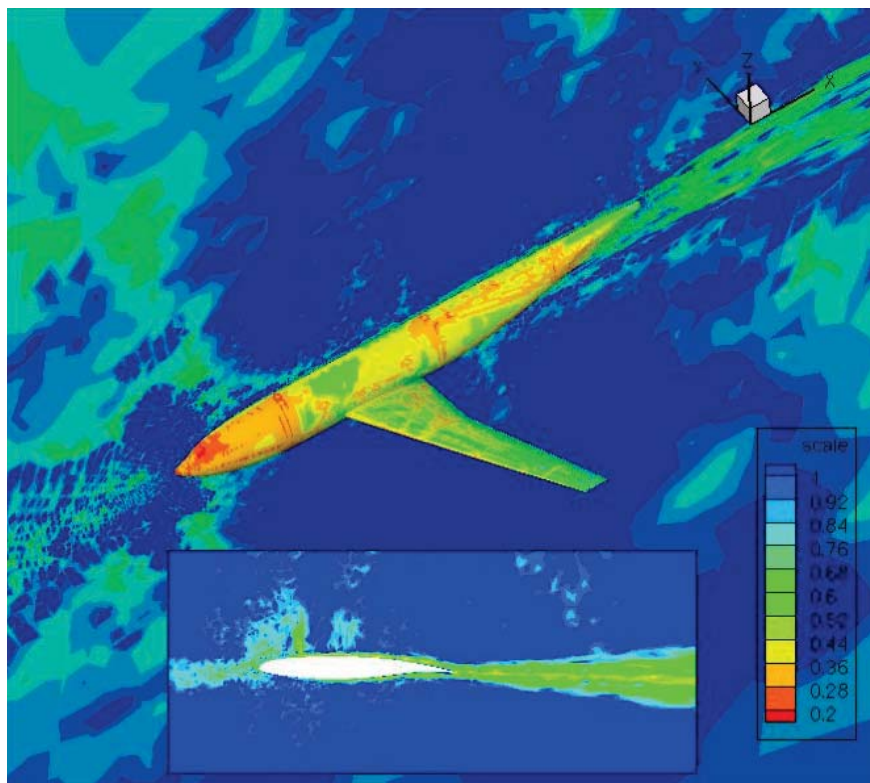


Figure 7: Adjoint-based adaptation parameter for the final medium-adapted mesh solution on the wing/body, symmetry plane and mid-span plane (inset) (from Lee-Rausch et al.<sup>40</sup>).

### Observations

The following observations can be made related to grids for transonic aerodynamic flows similar to the configurations tested in the various Drag Prediction Workshops.

1. Grid convergence on complex 3D problems is very difficult and probably requires more grid resolution than has been achieved in the DPW series.
2. Grid resolution requirements involving regions of separated flow are much more demanding and less well understood than attached flow.<sup>28</sup>
3. Generation of consistent grid families in the presence of complex geometries is a non-trivial task.<sup>28</sup>
4. Grid effects are most likely the dominant source of uncertainty.
  - (a) Perform grid convergence studies for the chosen problem.
    - i. Use uniform refinement and measure compliance of grids using a method such as Ollivier-Gooch<sup>36</sup> or Cavallo and Feldman.<sup>38</sup>
    - ii. Calculate the power of the convergence series by using the approach of Baker.<sup>25</sup>
    - iii. Compare the calculated convergence rate to the design order of the scheme. Identify deficiencies in the grid sequence, etc. and refine until the measured order of accuracy equals the design order.

- (b) Use gridding guidelines determined from best practices of expert practitioners. Refine the gridding guidelines.
5. For steady solutions, fully converge results to steady state and report the level of convergence. Converge at least four orders of magnitude but preferably to machine zero. For unsteady problems, use a temporal error controller.
6. Report figures of merit to sufficient accuracy for both computational and experimental results.

## B. Physical Modeling

Three approximations to the wind tunnel experiment have consistently been used in the DPW series. First, since many CFD codes did not include transition prediction capability or transition specification capability, all required cases were modeled as fully turbulent. Each turbulence model has its own numerical transition behavior and will reach a fully developed turbulent condition at a location that depends on the initial turbulence levels and numerical dissipation. DPW-II included an optional case to evaluate the effects of fixing transition at the location specified in the wind tunnel experiment. However, the individual fully turbulent results were never evaluated to identify where transition occurred. Additionally, sensitivity to the initial turbulence levels was never evaluated. For validation, transition should be modeled based on the validation experiment.

Second, the wind tunnel model is flexible and deflects under load; but to reduce the workload on grid generation and the participants, a single geometric definition for the configurations was used. DPW-II and DPW-III developed a finite element model of the DLR-F6 wind tunnel model and used the estimated deflection of the wind tunnel model at the design condition. DPW-IV and DPW-V also had a finite element model developed for the CRM wind tunnel model and used the estimated deflection of the wind tunnel model at the design condition. The experimental study for the CRM included photogrammetric measurement of the wind tunnel model during the test. This deflection data was compared to the estimated shape, and helped to identify that the wind tunnel model shape was different from the shape that was used for CFD in the workshops.<sup>41,42</sup>

Rivers et al.<sup>42</sup> studied the effect of the as-built wind tunnel model, the aeroelastic deflection, and the mounting system. Figure 8 shows the experimental data from both the NTF and the Ames tunnel tests, the DPW-V participant data, calculations with the aeroelastically-deflected wind tunnel model shape, and calculations with the sting mounting system added to the aeroelastic geometry. Each of the corrections improves the correlation of the prediction with the experimental data. The lift and drag coefficients show substantially closer agreement than the moment coefficient, but all show marked improvements when these effects are modeled. Additional studies<sup>43</sup> have confirmed that correcting the CFD model shape reduces the offset between CFD predictions and the wind tunnel data. The differences between the computational model and the wind tunnel model geometry will increase away from the design condition as the wind tunnel model deflection depends on the load and the CFD model was chosen to remain fixed throughout the workshop results.

Third, wind tunnel data is typically provided with one or more corrections applied to correct from wind tunnel conditions to a free air condition. These corrections may include wind tunnel wall corrections, buoyancy corrections, sting effects, etc. Rivers<sup>42</sup> demonstrated that including sting effects in calculations improves comparisons between the CFD predictions and wind tunnel data for the CRM, which did not include any sting effect corrections to the data. Pfeiffer<sup>44</sup> provided a review of DPW-II results and discussed the wind tunnel installation and sting effects. He identified a testing plan that would allow for experimental determination of sting effects. However, this testing has not been attempted on any of the results used in the Drag Prediction Workshops.

These three approximations to the physical modeling of the wind tunnel test limit the comparisons that can be made with the experimental data, and one should expect the predictions to show an offset from the experimental data due to these approximations. These approximations prevent the computations from being validated with the wind tunnel data.

Figure 9 shows the pitching moment curves for the CRM wing-body and wing-body-horizontal tail at three tail incidence settings from DPW-IV. The  $C_M$  curves break between 3° and 4° for both the wing-body and the wing-body-horizontal tail. Most of the predictions break to the left (unstable). However, some of the predictions break to the right (more stable). Vassberg et al.<sup>14</sup> hypothesize that the curves breaking unstable correspond to outboard wing stall, while those breaking more stable probably predict a rapid increase in the size of body separation bubble. The CRM wing geometry was designed with an aggressive upper surface pressure gradient at the outboard section of the wing, which would lead to trailing edge separation.<sup>16</sup> As such, the test case was well designed to create a case to differentiate between model predictions. Further details of the predictions would be required to correlate the separation zones with the moment behavior, and more experimental data is required to identify the physical cause of the pitching moment break. Currently there is not sufficient experimental data to identify which, if either, behavior is correct.

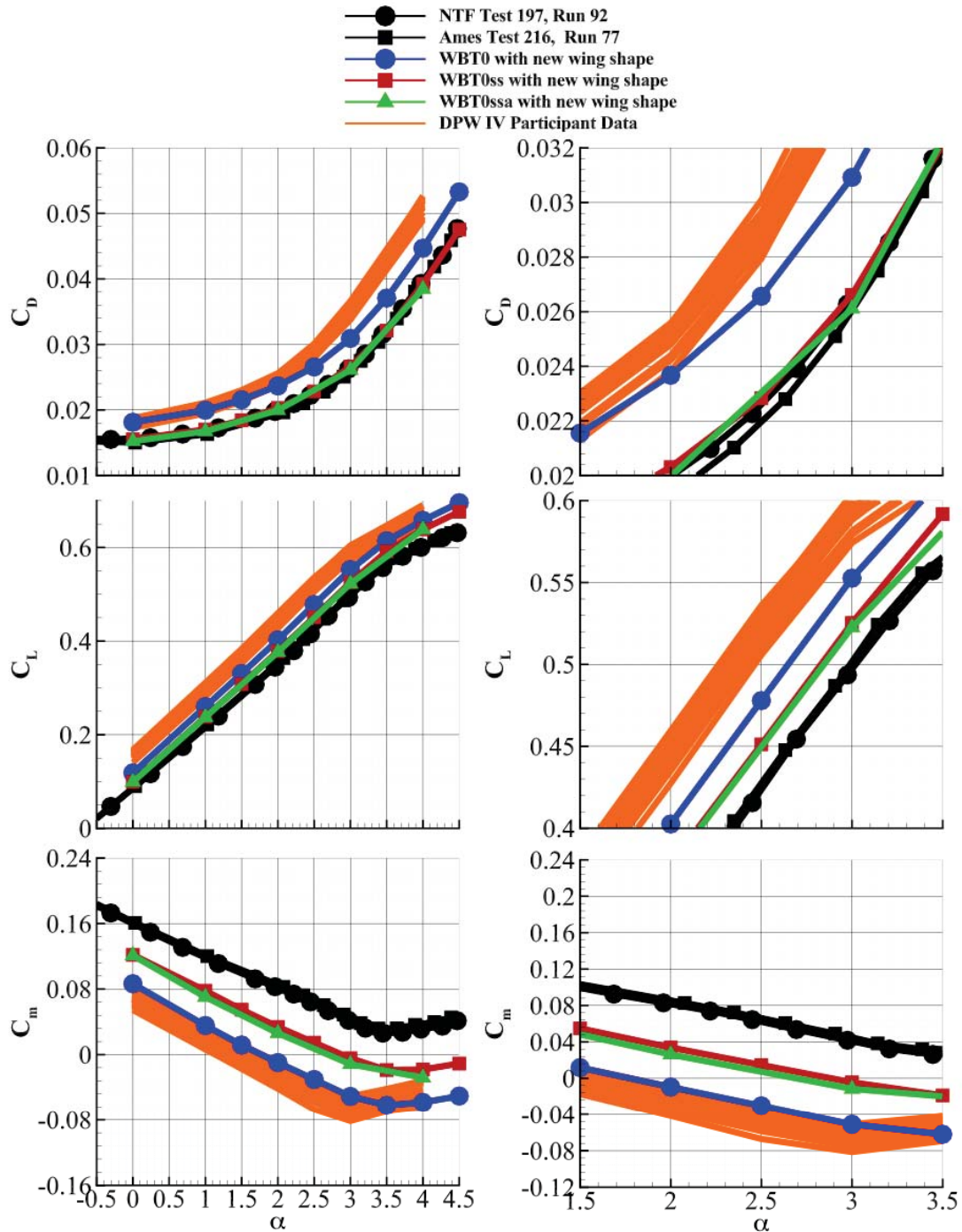


Figure 8: Comparison of NTF and Ames 11-ft TWT experimental data with the DPW-IV CRM CFD data for the wing-body-horizontal tail,  $i_H = 0^\circ$ , (WBT0) configuration along with the USM3D CFD data for the WBT0ss (wing-body-horizontal tail with support system) and WBT0ssa (wing-body-horizontal tail with support system and arc sector) configurations using the new wing shape,  $M = 0.85$ ,  $Re = 5 \times 10^6$  (from Rivers et al.<sup>42</sup>).

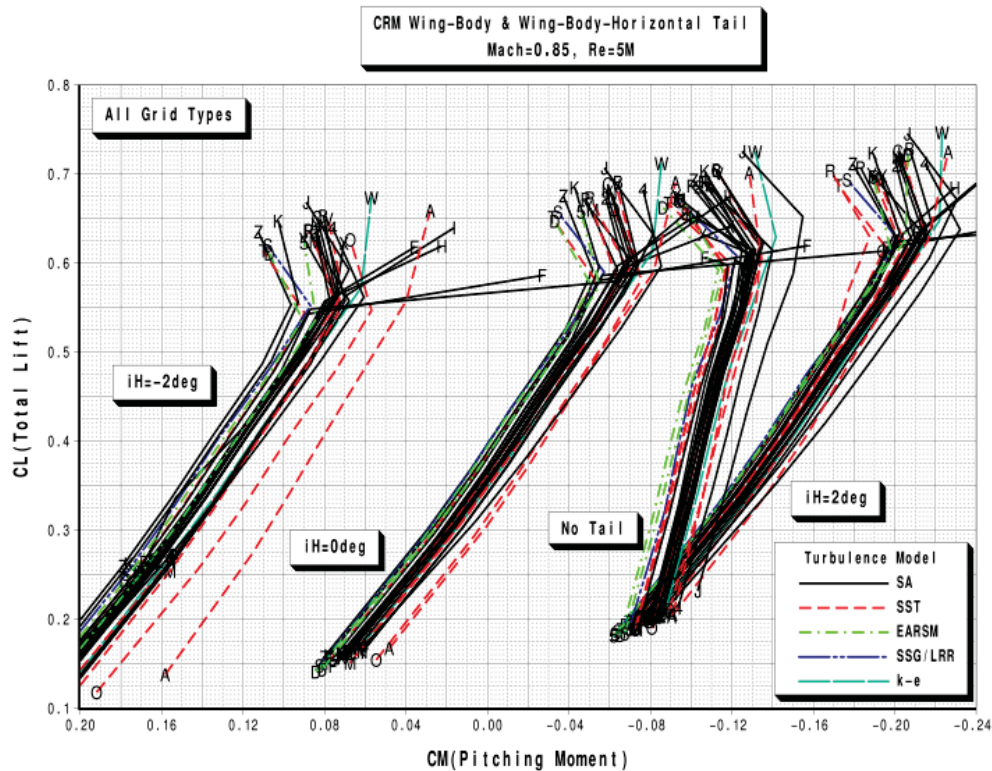


Figure 9: DPW-IV CRM pitching moment curves (from Vassberg et al.<sup>14</sup>).

DPW-V included a turbulence model verification study<sup>21</sup> designed to determine if a given turbulence model was implemented in a CFD code as intended. There were three 2D cases provided from the Turbulence Model Resource website.<sup>45</sup> The verification test identified a discrepancy in the calculation of the minimum distance to the wall on a 2D bump case from at least one participant. This discrepancy affected the skin friction prediction of the SA model. A correction to the wall distance calculation was implemented, and the prediction then matched the expected result. Additionally, the particular version of the SST model made a difference in the skin friction results. These differences are almost impossible to identify in a complex problem where there could be many differences in modeling the problem<sup>46</sup> and where obtaining a grid converged solution is very difficult. Therefore, verification studies on simpler problems are critical to identify differences in numerical implementation. Additionally, many participants reported few details of their turbulence model. The Turbulence Model Resource Website includes standardized nomenclature of variations of turbulence models. This nomenclature should be used to clearly identify which turbulence model(s) the participant is using. Additional details of numerical implementation should also be included as they can often affect the results.

Murayama et al.<sup>47</sup> investigated the effects of turbulence modeling for the DPW-V CRM wing-body configuration buffet onset case. The SA turbulence model predicted slightly larger the side of body separation than the SST turbulence model on a series of coarse, medium, and fine multiblock grids. The SST model actually showed no separation on the coarse grid while the SA showed separation similar in size to the fine grid. Clearly the coarse grid is not in the asymptotic range for the SST model. The SA model using the QCR (Quadratic Constitutive Relationship), which replaces the linear stress-strain Boussinesq relationship, predicted no separation for the same case. Figure 10 shows the surface-restricted streamlines on the wing surface for the SA turbulence model with and without the QCR model. The shock induced separation at the mid-span area increases with the QCR. However, there is no experimental data available to validate that the details of the flow prediction are correct.

For DPW-V, Levy et al.<sup>21</sup> identified significant variation in lift and pitching moment in the buffet onset solutions at each angle of attack that were driven largely by shock location and the amount of trailing edge separation. Figure 11 shows that there is massive separation by 4° angle of attack, and the separation exhibits significantly different patterns between solutions. There is no discernible trend. Levy et al.<sup>21</sup> raised the question whether this chaotic situation at the high angles of attack might be physical as well as computational. Are the steady Reynolds-averaged Navier-Stokes equations appropriate for modeling this flow regime?

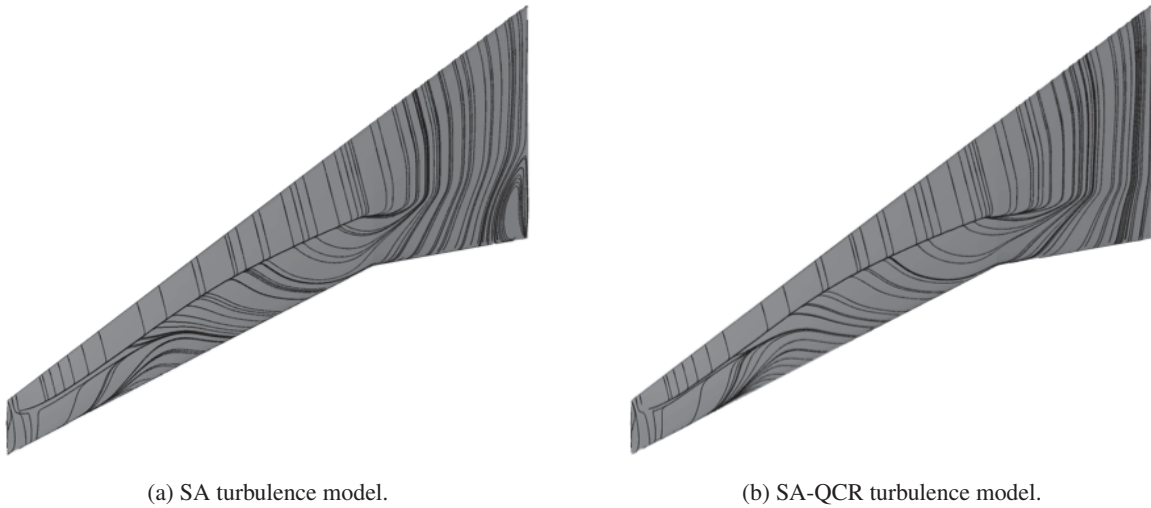


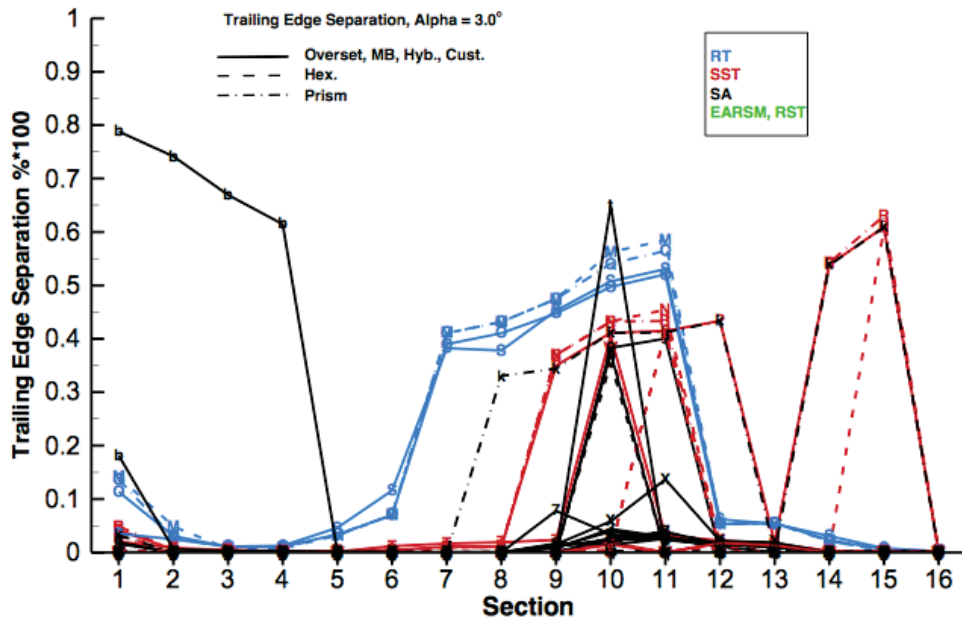
Figure 10: Comparison of surface-restricted streamlines on the DPW-V CRM wing-body configuration wing surface with the SA turbulence model and the SA turbulence model with the QCR modification. Calculations using the UPACS code on the L3 medium common multi-block grid at  $M = 0.85$ ,  $Re = 5 \times 10^6$ ,  $4^\circ$  angle of attack (from Murayama et al.<sup>45</sup>).

Extensive validation experiments with detailed flow physics measurements are required to address several of these physical modeling issues. These experiments need to be designed to isolate effects and measure data that will distinguish between models.

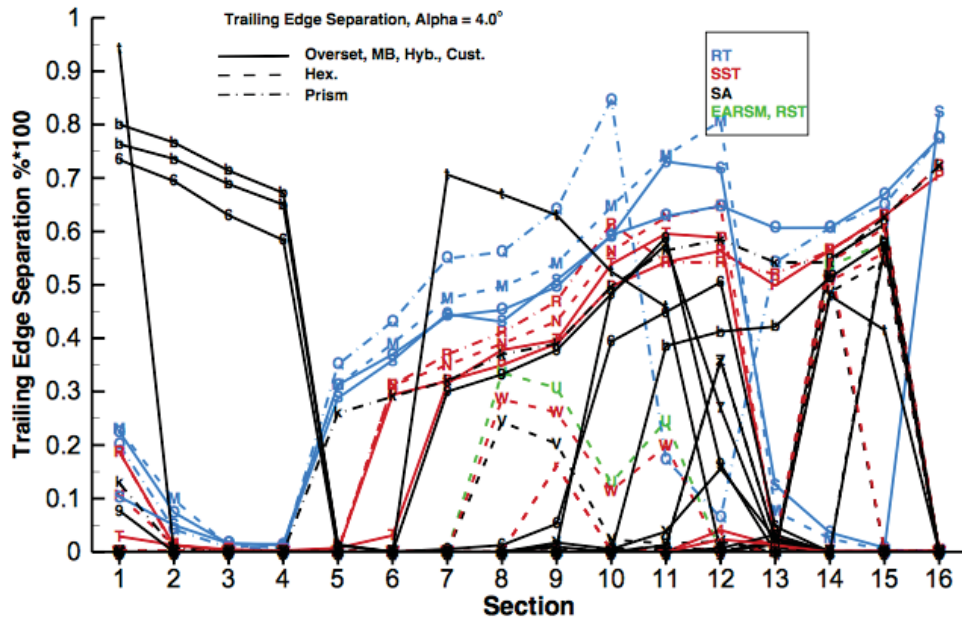
#### Observations

The following observations can be made related to physical modeling for transonic aerodynamic flows similar to the configurations tested in the various Drag Prediction Workshops.

1. Flow separation is challenging to simulate.
2. Perform code verification first. Use simple cases to verify implementation of physical models.
3. Report details of the turbulence model, or use common nomenclature<sup>45</sup> when reporting which model.
4. Provide a series of cases with increasing complexity. Realistic configurations are very complex with unexpected areas of separation, etc. where many effects are confounded. Identify simpler cases to isolate the effects.
5. Collect experimental data to distinguish effects, e.g., transition location, separation, Reynolds number effects.
6. Raw experimental data plus all recommended wind tunnel corrections should be provided to the participants to permit an independent assessment of experimental error.<sup>30,44</sup>
7. Measure the geometry of the wind tunnel model before, during, and after the test.<sup>30</sup>
8. If simplifying assumptions are required, provide a method of evaluating sensitivity to those assumptions, e.g., fully turbulent.



(a) 3° angle of attack.



(b) 4° angle of attack.

Figure 11: Trailing edge separation on CRM at 3° and 4° angle of attack from DPW-V (from Levy et al.<sup>21</sup>).

### C. Open Forum

Each workshop had standard grids generated for multi-block, overset, and unstructured grids. Beginning with DPW-II, these grids are distributed via the Internet and the organizers maintained a web site with the grids available. The hope was that these grids would continue to be used by other researchers. Participants were always encouraged to develop their own grids in addition to using the mandatory grids. However, beginning with DPW-III, participants who used their own grids were required to make these grids available via the DPW web site for others to use. This allows participants to evaluate effects of grids on solutions.

The decision to keep grids available has proven to be an excellent decision. The organizing committee has continuously been impressed with the amount of work that participants and other researchers are willing to do both for the workshops and well after the workshop. Participants and other researchers across the world continue to download grids from the workshops and run additional cases. New papers using these grids and results from previous workshops show up at many conferences. Each of these studies add to the body of results and increases our understanding of CFD predictive capability.

The workshops have proven to be a very rich environment. Extensive discussions have been held in each workshop to identify trends and problems.

#### *Observations*

Workshops provide an excellent mechanism to bring many people together to focus on a problem and to address issues in how the problem is solved that does not happen in individual paper based results.

1. Make all grids available to participants—this allows participants to run grids used with other solvers to evaluate the effect of the grids on the solutions.
2. Make all results available for others to analyze.

## IV. Validation Experiments

As mentioned in the previous section, improving physical models requires not only insights to enable model creation but also very carefully executed experiments to validate those physical models. In this section we explore the lessons learned during a recent validation experiment campaign for supersonic retropropulsion (SRP)<sup>48–50</sup> and review some of the recommendation for conducting such a validation experiment as espoused by Oberkampf et al.<sup>1,51,52</sup>

In 2010, SRP (firing jets into the oncoming supersonic flow as a means of deceleration) was identified as an essential technology for five of nine entry, decent, and landing architectures studied for humans Mars exploration.<sup>53</sup> Due to the nascent state of the SRP technology and the lack of ground test facilities to simulate Martian atmospheric conditions, a campaign was launched to begin validating CFD as a tool for predicting SRP environments. The first step was to conduct a validation experiment of a simple SRP model in air with non-reacting jets because as Ref. 51 describes, “the common practice of attempting to validate codes using published data obtained for some purpose unrelated to code validation” was found to be unsatisfactory. Previous SRP experimental test campaigns were conducted in the 1960s and 1970s; but because they were not designed and conducted as CFD validation experiments, they were unusable for CFD validation. The most frequent shortcomings of these early experiments were the lack of input characterization, e.g., freestream temperature or jet plenum temperature, a lack of detailed geometry, and complete absence of rigorous uncertainty quantification. Refs. 48 and 49 document the collaborative SRP validation experiment design, and here we will only highlight some of the insights and issues uncovered and during that process.

First and foremost was the mantra, “*Metior totum. Interrogo totum.*” (Measure everything. Question everything.) For example, due to concerns regarding heat conduction and possible acoustic resonance in the jet plenums, the SRP experiment not only had temperature and pressure measurements for the main jet plenum manifold but also measurements just upstream of the individual jet nozzles and all were high-frequency transducers.

One of the first steps of the SRP experimental design was to size the model to minimize tunnel wall interference by running preliminary CFD computations that compared the model surface pressure effects between enclosed (tunnel) and open (ideal) domains. Meanwhile, the wind tunnel from the plenum through the diffuser was digitized in case the full flow path needed to be modeled.

Validation experiments are expensive. Do not under sell the test campaign to get your foot in the door. Be explicit and upfront with cost estimates for the extensive test matrix necessary to obtain quantified experimental uncertainties—see Ref. 51. Also, set clear, prioritized goals to maintain the focus on CFD validation. During the SRP validation

experiment campaign, the CFD validation goal was often overshadowed by desires to explore more jet and vehicle configurations, to make the experiment more flight-relevant, or to cut costs.

Another insight was to avoid physics that are not essential to the problem under study. Search for the simplest problem that still contains the desired physics. If you can minimize the extent of separation, unsteady flow, shocks, and turbulent flow, do so. For example, the jet plenum air was heated to avoid jet plume liquefaction because condensation physics was not the focus of the validation effort or a consideration in the final application with reacting jets. And because the plenum air was heated, Berry et al.<sup>48</sup> further determined that to avoid heat conduction effects (loss of jet total temperature), heat-soaking the model prior to taking data was essential to keep the modeling as simple as possible. Similarly, if your problem involves turbulent flow, use trips as necessary to ensure transition (and preferably trips that can be readily modeled if necessary). Also, take care to choose designs that will not tend to re-laminarize. For example, add a fuselage/wing root leading edge horn so the turbulent flow along the fuselage remains so as it transitions onto the wing leading edge.

Strive for as much symmetry as possible and keep the geometry as simple as possible. One of the SRP configurations had a central jet, so the model was axisymmetric (and indeed one of the experimental runs revealed a predominantly axisymmetric jet interaction mode). The other jet configurations had 120-degree symmetries (three nozzles). Other simplifications include making the nozzles conical instead of bell-shaped and enclosing the after body of the model in a cylindrical housing. In retrospect, one mistake was not adding an additional fairing to simplify modeling the high pressure line and instrumentation cables exiting the back of the model along the sting. After seeing the model mounted in the tunnel, photographs were taken; and a rough numerical model was created and simulated to gauge the effects of these excrescences. The deltas between ideal (clean) and as-tested were noticeable but thankfully their effects were confined to the rear of the model and away from the primary jet interaction region at the front.

Try to establish a hierarchy of comparisons, starting with the simplest/easiest first. For example: a) body forces and moments; b) control surface forces and moments; c) surface pressure distributions; d) surface heat flux and shear stress; e) flowfield distributions of pressure, temperature, and velocity components; and f) flowfield distributions of Reynolds stresses. For the SRP validation experiment, a flow-through balance was not available to acquire integrated forces and moments, but the experiment did have extensive surface pressure measurements, a host of model and plenum temperature measurements, and high-speed schlieren videos.

CFD cases computed prior to the tunnel entry allowed the use of the Virtual Diagnostics Interface (ViDI) methodology<sup>54-56</sup> to display comparisons of pre-computed and live, experimentally-measured, surface pressures. This provided a rapid, in situ, check of pressure tap mapping and calibration; and also allowed rapid identification of bad data channels and tunnel interference effects as the model was traversed throughout the test section to collect measurements in support of statistical measurement uncertainty quantification. For the initial smooth forebody, no-jet cases, laminar CFD runs were used to double check the experimental data reduction system. Upon entering a new tunnel, an error was found in the data reduction algorithms thanks to this synergy between CFD and experiment.

### *Observations*

The lessons learned during the validation experiment described above, fully support the following guidelines for conducting validation experiments from Ref. 48 and should be used when conducting validation experiments for transonic aerodynamic flows similar to the configurations tested in the various Drag Prediction Workshops.

1. A validation experiment should be jointly designed by experimentalists, model developers, code developers, and code users closely together throughout the program, from inception to documentation, with complete candor about the strengths and weaknesses of each approach.
2. A validation experiment should be designed to capture the essential physics of interest, and measure all relevant physical modeling data, initial and boundary conditions, and system excitation information required by the model.
3. A validation experiment should strive to emphasize the inherent synergism that is attainable between computational and experimental approaches.
4. Although the experimental design should be developed cooperatively, independence must be maintained in obtaining the computational and experimental system response results.
5. Experimental measurements should be made of a hierarchy of system response quantities, for example, from globally integrated quantities to local quantities.

6. The experimental design should be constructed to analyze and estimate the components of random (precision) and systematic (bias) experimental uncertainties.

## V. Concluding Remarks

The past decade of AIAA Drag Prediction Workshops and a recent validation experiment were mined for lessons learned to improve future workshops and associated experiments. These lessons were grouped into four areas: grid and numerical approximations, physical modeling, open forums, and validation experiments. Within each area several case studies were provided and followed by a summary list of observations for each area. For the grid and numerical approximation area, techniques for creating proper grid families were paramount. In the physical modeling area, the need for focused, validation experiments was evident while the open forum category underscored the multiplying power of open, transparent, communication. Finally, the validation experiments section underscored the benefits of following the guidelines developed by Oberkampf et al.<sup>1,48,51,52</sup>

Overarching observations include: 1) due to simplifications in the workshop test cases, wind tunnel data are not necessarily the “correct” results that CFD should match, 2) an average of core CFD data are not necessarily a better estimate of the true solution as it is merely an average of other solutions and has many coupled sources of variation, 3) outlier solutions should be investigated and understood, and 4) the DPW series does not have the systematic build up and definition on both the computational and experimental side that is required for detailed verification and validation.

## Acknowledgments

The authors would like to thank all the participants of the five Drag Prediction Workshops who have provided tremendous time and effort to make these a success. The authors thank P. Eliasson, E. Lee-Rausch, D. Levy, M. Murayama, M. Park, M. Rivers, and C. Rumsey. The authors wish to thank the AIAA Applied Aero Technical Committee for their continued support of DPW over more than a decade. The authors wish to thank the AIAA Meshing, Visualization, and Compute Environments Technical Committee for many grid related discussions and assistance in understanding the influence of grids.

## References

- <sup>1</sup>Oberkampf, W. L. and Roy, C. J., *Verification and Validation in Scientific Computing*, Cambridge University Press, Cambridge, UK, 2010.
- <sup>2</sup>Levy, D. W., Zickuhr, T., Vassberg, J., Agrawal, S., Wahls, R. A., Pirzadeh, S., and Hemsch, M. J., “Data Summary from the First AIAA Computational Fluid Dynamics Drag Prediction Workshop,” *Journal of Aircraft*, Vol. 40, No. 5, 2003, pp. 875–882.
- <sup>3</sup>Hemsch, M. J., “Statistical Analysis of Computational Fluid Dynamics Solutions from the Drag Prediction Workshop,” *Journal of Aircraft*, Vol. 41, No. 1, 2004, pp. 95–103.
- <sup>4</sup>Redeker, G., “DLR-F4 Wing Body Configuration,” *A Selection of Experimental Test Cases for the Validation of CFD Codes*, AGARD-AR-303 Vol. II, August 1994, pp. B4.1–B4.21.
- <sup>5</sup>Redeker, G., Muller, R., Ashill, P. R., Elsenaar, A., and Schmitt, V., “Experiments on the DLR-F4 Wing Body Configuration in Several European Wind Tunnels,” *Aerodynamic Data Accuracy and Quality: Requirements and Capabilities in Wind Tunnel Testing*, Chapter 2, AGARD-CP-429, July 1988.
- <sup>6</sup>Elsholz, E., “The DLR-F4 Wing/Body Configuration,” *ECARP—European Computational Aerodynamics Research Project: Validation of Turbulence Models*, Vol. 58 of *Notes on Numerical Fluid Mechanics*, 1997, pp. 429–459.
- <sup>7</sup>Laffin, K. R., Klausmeyer, S. M., Zickuhr, T., Vassberg, J. C., Wahls, R. A., Morrison, J. H., Brodersen, O. P., Rakowitz, M. E., Tinoco, E. N., and Godard, J.-L., “Data Summary from Second AIAA Computational Fluid Dynamics Drag Prediction Workshop,” *Journal of Aircraft*, Vol. 42, No. 5, 2005, pp. 1165–1178.
- <sup>8</sup>Hemsch, M. J. and Morrison, J. H., “Statistical Analysis of CFD Solutions from 2nd Drag Prediction Workshop,” AIAA Paper 2004-0556, January 2004.
- <sup>9</sup>Brodersen, O. and Sturmer, A., “Drag Prediction of Engine-Airframe Interference Effects Using Unstructured Navier-Stokes Calculations,” AIAA Paper 2001-2414, June 2001.
- <sup>10</sup>Morrison, J. H. and Hemsch, M. J., “Statistical Analysis of CFD Solutions from the Third AIAA Drag Prediction Workshop,” AIAA Paper 2007-0254, January 2007.
- <sup>11</sup>Vassberg, J. C., Sclafani, A. J., and DeHaan, M. A., “A Wing-Body Fairing Design for the DLR-F6 Model: a DPW-III Case Study,” AIAA Paper 2005-4730, June 2005.
- <sup>12</sup>Vassberg, J. C., Tinoco, E. N., Mani, M., Brodersen, O. P., Eisfeld, B., Wahls, R. A., Morrison, J. H., Zickuhr, T., Laffin, K. R., and Mavriplis, D. J., “Summary of the Third AIAA CFD Drag Prediction Workshop,” AIAA Paper 2007-0260, January 2007.
- <sup>13</sup>Gatlin, G. M., Rivers, M. B., Goodliff, S. L., Rudnik, R., and Sitzmann, M., “Experimental Investigation of the DLR-F6 Transport Configuration in the National Transonic Facility (Invited),” AIAA Paper 2008-6917, August 2008.
- <sup>14</sup>Vassberg, J. C., Tinoco, E. N., Mani, M., Zickuhr, T., Levy, D. W., Brodersen, O. P., Eisfeld, B., Wahls, R. A., Morrison, J. H., Mavriplis, D. J., and Murayama, M., “Summary of the Fourth AIAA CFD Drag Prediction Workshop,” AIAA Paper 2010-4547, June 2010.

- <sup>15</sup>Morrison, J. H., "Statistical Analysis of CFD Solutions from the Fourth AIAA Drag Prediction Workshop," AIAA Paper 2010-4673, June 2010.
- <sup>16</sup>Vassberg, J. C., DeHaan, M. A., Rivers, S. M., and Wahls, R. A., "Development of a Common Research Model for Applied CFD Validation Studies," AIAA Paper 2008-6919, August 2008.
- <sup>17</sup>Rivers, M. and Dittberner, A., "Experimental Investigations of the NASA Common Research Model (Invited)," AIAA Paper 2010-4218, June 2010.
- <sup>18</sup>Rivers, M. and Dittberner, A., "Experimental Investigations of the NASA Common Research Model in the NASA Langley National Transonic Facility and NASA Ames 11-ft Transonic Wind Tunnel (Invited)," AIAA Paper 2011-1126, January 2011.
- <sup>19</sup>Vassberg, J. C., "A Unified Baseline Grid about the Common Research Model Wing-Body for the Fifth AIAA CFD Drag Prediction Workshop," AIAA Paper 2011-3508, June 2011.
- <sup>20</sup>Morrison, J. H., "Statistical Analysis of CFD Solutions from the Fifth AIAA Drag Prediction Workshop," AIAA Paper 2013-0047, January 2013.
- <sup>21</sup>Levy, D. W., Lafin, K. R., Tinoco, E. N., Vassberg, J. C., Mani, M., Rider, B., Rumsey, C., Wahls, R. A., Morrison, J. H., Brodersen, O. P., Crippa, S., Mavriplis, D. J., and Murayama, M., "Summary of Data from the Fifth AIAA CFD Drag Prediction Workshop," AIAA Paper 2013-0046, January 2013.
- <sup>22</sup><http://aaac.larc.nasa.gov/tsab/cfdlarc/aiaa-dpw/> [cited 10 December 2013].
- <sup>23</sup>Salas, M. D., "Digital Flight: The Last CFD Aeronautical Grand Challenge," *Journal of Scientific Computing*, Vol. 28, No. 2/3, 2006, pp. 479–505.
- <sup>24</sup>Salas, M. D., "Some Observations on Grid Convergence," *Computers & Fluids*, Vol. 35, No. 7, 2006, pp. 688–692.
- <sup>25</sup>Baker, T. J., "On the Relationship between Mesh Refinement and Solution Accuracy," AIAA Paper 2005-4875, June 2005.
- <sup>26</sup>Turgeon, E., Pelletier, D., and Ignat, L., "Effects of Adaptivity on Various Finite Element Schemes for Turbulent Heat Transfer and Fluid Flow," *Numerical Heat Transfer: Applications*, Vol. 38, No. 12, 2000, pp. 847–868.
- <sup>27</sup>Pelletier, D., "DPW: Reflections from an outsider. Or The RANS' elusive asymptotic range!" AIAA Paper 2008-6922, August 2008.
- <sup>28</sup>Mavriplis, D. J., Vassberg, J. C., Tinoco, E. N., Mani, M., Brodersen, O. P., Eisfeld, B., Wahls, R. A., Morrison, J. H., Zickuhr, T., Levy, D., and Murayama, M., "Grid Quality and Resolution Issues from the Drag Prediction Workshop Series," *Journal of Aircraft*, Vol. 46, No. 3, May-June 2009, pp. 935–950.
- <sup>29</sup>Mavriplis, D. J., "Grid Resolution Study of a Drag Prediction Workshop Configuration Using the NSU3D Unstructured Mesh Solver," AIAA Paper 2005-4729, June 2005.
- <sup>30</sup>Baker, T. J., "Parsing the Results of the Second Drag Prediction Workshop," AIAA Paper 2005-4731, June 2005.
- <sup>31</sup>Eliasson, P. and Peng, S.-H., "Drag Prediction for the DLR-F6 Wing-Body Configuration Using the Edge Solver," *Journal of Aircraft*, Vol. 45, No. 3, May-June 2008, pp. 837–847.
- <sup>32</sup>Scalafani, A. J., Vassberg, J. C., Harrison, N. A., Rumsey, C. L., Rivers, S. M., and Morrison, J. H., "CFL3D/OVERFLOW Results for DLR-F6 Wing/Body and Drag Prediction Workshop Wing," *Journal of Aircraft*, Vol. 45, No. 3, May-June 2008, pp. 762–780.
- <sup>33</sup>Tinoco, E. N., Venkatakrishnan, V., Winkler, C., and Mani, M., "Structured and Unstructured Navier-Stokes Solvers for the Third Drag Prediction Workshop," *Journal of Aircraft*, Vol. 45, No. 3, May-June 2008, pp. 738–749.
- <sup>34</sup>Murayama, M. and Yamamoto, K., "Comparison of Drag Prediction by Structured and Unstructured Mesh Method," *Journal of Aircraft*, Vol. 45, No. 3, May-June 2008, pp. 799–822.
- <sup>35</sup>Mavriplis, D., "Third Drag Prediction Workshop Results Using the NSU3D Unstructured Mesh Solver," *Journal of Aircraft*, Vol. 45, No. 3, May-June 2008, pp. 750–761.
- <sup>36</sup>Ollivier-Gooch, C., "Assessing Validity of Mesh Refinement Sequences with Application to DPW-III Meshes," AIAA Paper 2009-1174, January 2009.
- <sup>37</sup>Dannenhoffer, III, J. F., "Correlation of Grid Quality Metrics and Solution Accuracy for Supersonic Flows," AIAA Paper 2012-0610, January 2012.
- <sup>38</sup>Cavallo, P. A. and Feldman, G. M., "Correlation of Grid and Solution Pairs Using Metric Tensor Intersections," AIAA Paper 2013-0704, January 2013.
- <sup>39</sup>Vos, J. B., Sanchi, S., and Gehri, A., "Drag Prediction Workshop 4 Results Using Different Grids Including Near-Field/Far-Field Drag Analysis," *Journal of Aircraft*, Vol. 50, No. 5, September-October 2013, pp. 1615–1627.
- <sup>40</sup>Lee-Rausch, E., Park, M., Jones, W., Hammond, D., and Nielsen, E., "Application of Parallel Adjoint-Based Error Estimation and Anisotropic Grid Adaptation for Three-Dimensional Aerospace Configurations," AIAA Paper 2005-4842, June 2005.
- <sup>41</sup>Rivers, M. B. and Hunter, C. A., "Support System Effects on the NASA Common Research Model," AIAA Paper 2012-0707, January 2012.
- <sup>42</sup>Rivers, M. B., Hunter, C. A., and Campbell, R. L., "Further Investigation of the Support System Effects and Wing Twist on the NASA Common Research Model," AIAA Paper 2012-3209, June 2012.
- <sup>43</sup>Hue, D., "CFD Investigations on the DPW-5 Configuration with Measured Experimental Wing Twist using the elsA Solver and the Far-Field Approach," AIAA Paper 2013-2508, June 2013.
- <sup>44</sup>Pfeiffer, N. J., "Reflections on the Second Drag Prediction Workshop," AIAA Paper 2004-0557, January 2004.
- <sup>45</sup><http://turbmodels.larc.nasa.gov> [cited 10 December 2013].
- <sup>46</sup>Kleb, B. and Wood, B., "CFD: A Castle in the Sand?" AIAA Paper 2004-2627, June 2004.
- <sup>47</sup>Murayama, M., Yamamoto, K., Hashimoto, A., Ishida, T., Ueno, M., Tanaka, K., and Ito, Y., "Summary of JAXA Studies for the Fifth AIAA CFD Drag Prediction Workshop Using UPACS and FaSTAR," AIAA Paper 2013-0049, January 2013.
- <sup>48</sup>Berry, S. A., Laws, C. T., Kleb, W. L., Rhode, M. N., Spells, C., McCrea, A. C., Trumble, K. A., Schauerhamer, D. G., and Oberkampf, W. L., "Supersonic Retro-Propulsion Experimental Design for Computational Fluid Dynamics Model Validation," IEEEAE Paper 1499, March 2011.
- <sup>49</sup>Trumble, K. A., Schauerhamer, D. G., Kleb, W. L., and Edquist, K. T., "Analysis of Navier-Stokes Codes Applied to Supersonic Retro-Propulsion Wind Tunnel Test," IEEEAE Paper 1471, March 2011.
- <sup>50</sup>Kleb, W. L., Schauerhamer, D. G., Trumble, K. A., Sozer, E., Barnhardt, M., Carlson, J.-R., and Edquist, K. T., "Toward Supersonic Retropropulsion CFD Validation," AIAA Paper 2011-3490, June 2011.

<sup>51</sup>Aeschliman, D. P. and Oberkampf, W. L., “Experimental Methodology for Computational Fluid Dynamics Code Validation,” *AIAA Journal*, Vol. 36, No. 5, 1998, pp. 733–741.

<sup>52</sup>Oberkampf, W. L. and Trucano, T. G., “Verification and Validation in Computational Fluid Dynamics,” *Progress in Aerospace Sciences*, Vol. 38, No. 3, 2002, pp. 209–272.

<sup>53</sup>Dwyer Cianciolo, A. M., Davis, J. L., Komar, D. R., Munk, M. M., Samareh, J. A., Williams-Byrd, J. A., Zang, T. A., Powell, R. W., Shidler, J. D., Stanley, D. O., Wilhite, A. W., Kinney, D. J., McGuire, M. K., Arnold, J. O., Howard, A. R., Sostaric, R. R., Studak, J. W., Zumwalt, C. H., Llama, E. G., Casoliva, J., Ivanov, M. C., Clark, I., and Sengupta, A., “Entry, Descent and Landing Systems Analysis Study: Phase 1 Report,” NASA TM 2010-216720, July 2010.

<sup>54</sup>Schwartz, R. J., “ViDI: Virtual Diagnostics Interface Volume 1—The Future of Wind Tunnel Testing,” NASA/CR 2003-212667, December 2003.

<sup>55</sup>Schwartz, R. J. and Fleming, G. A., “LiveView3D: Real Time Data Visualization for the Aerospace Testing Environment,” AIAA Paper 2006-1388, January 2006.

<sup>56</sup>Schwartz, R. J. and McCrea, A. C., “Virtual Diagnostic Interface: Aerospace Experimentation in The Synthetic Environment,” *MODSIM World 2009 Conference and Expo*, Virginia Beach, Virginia, October 2009.